Supplement of Biogeosciences, 15, 4459–4480, 2018
https://doi.org/10.5194/bg-15-4459-2018-supplement

Biogeosciences Open Access EGU

Supplement of

Global soil organic carbon removal by water erosion under climate change and land use change during AD 1850–2005

Victoria Naipal et al.

Correspondence to: Victoria Naipal (victoria.naipal@lsce.ipsl.fr)

S1 Derivation of RUSLE factors

The regression equations to calculate the R-factor operate on one or more of the following parameters: total annual precipitation, mean elevation, and the simple precipitation intensity index, SDII. SDII is calculated based on the hourly precipitation data from ISIMIP2B (Frieler et al., 2016), by dividing the total yearly precipitation by the total number of wet days (> 1mm) in a year. Mean elevation is derived from the 5 arcmin-resolution ETOPO data (National Geophysical Data Center/NESDIS/NOAA, 1995).

After calculating the R-factor for the year 2005AD using the above-mentioned data, we compared it to the high-resolution global erosivity dataset from Panagos *et al.* (2017). We find that our global erosivity map shows a similar spatial variability in erosivity as that from Panagos *et al.* (2017). There are regions where the erosivity values from our study are at the low side, such as the west coast of North-America, Australia and parts of Asia, which can be explained by missing extreme events (Fig. S1A & B).

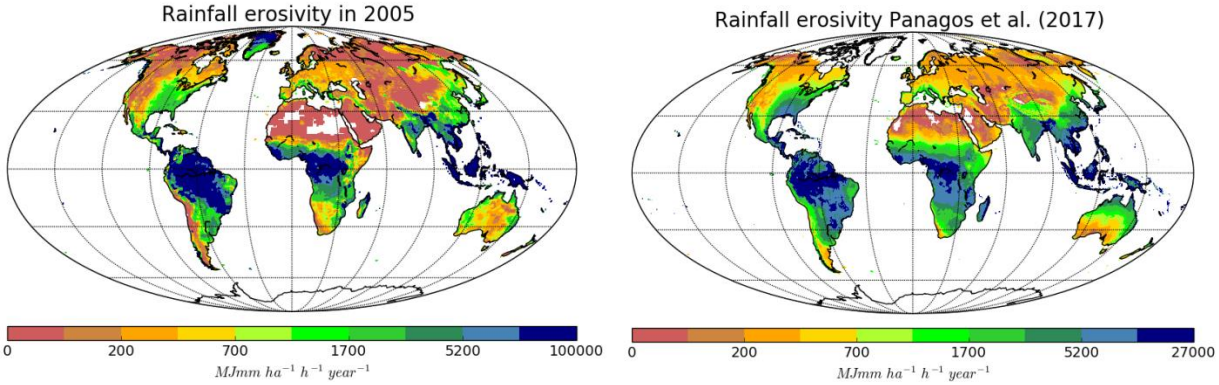

Figure S1: (A) Global rainfall erosivity from this study for the year 2005AD, and (B) global rainfall erosivity map derived from Panagos *et al.* (2017). Both maps have the resolution of 5 arcmin.

To account for the uncertainty in the R-factor we made the R-factor range between a minimum and maximum value using the uncertainty range in the regression parameters for each climate zone.

Due to the lack of data on the normalized difference vegetation index (NDVI), the method presented in the study of Naipal *et al.* (2015) for estimation of the C factor of the Adj.RUSLE model could not be used in this study. Instead, the method from the study of Naipal *et al.* (2016)was used. This method is based on the C values provided by Panagos *et al.* (2015) for Europe for different land cover types, combined with the leaf area index (LAI) from the ORCHIDEE model. The LAI is used to estimate the percentage vegetation cover (cf), which has been shown to influence the overall value of the C factor for a specific land cover type (Walter & Wischmeier, 1972). cf (dimensionless) is estimated according to the Beer's Law approximation:

$$cf = 1 - e^{-0.5*LAI} \quad (1)$$

Five cf classes are distinguished: cf > 0.75, 0.6<cf<=0.75, 0.45<cf<=0.6, 0.2<cf<=0.45 and cf<= 0.2. The corresponding C-factors for the different land cover types used in this study is given in table S1. If cf was smaller than 0.2, all land cover types, except bare soil, were given a maximum value of 0.45. This value corresponds to the

maximum C values found by United States Department of Agriculture (Walter & Wischmeier, 1972) and Panagos *et al.* (2015). For bare soil the maximum C value is 0.55, which is according to Panagos *et al.* (2015).

To account for the uncertainty in the C-factor we made the C-factor range between a minimum and maximum value based on the uncertainty range in the land-cover specific C values from literature.

cf	Forest	Grass	Crops	Bare
> 0.75	0.0001	0.01	0.03	0.1
0.6 - 0.75	0.00089	0.029	0.14	0.2
0.45 - 0.60	0.00168	0.048	0.26	0.29
0.20 - 0.45	0.003	0.08	0.45	0.45
< 0.20	0.45	0.45	0.45	0.55

Table S1: C values for different PFTs and cover fractions (cf)

The K-factor (t ha h ha^{-1} MJ^{-1} mm^{-1}) of the Adj.RUSLE model is calculated using 30 arcsec soil data on sand, silt, clay fractions and percent organic matter (from Global Soil Data set for use in Earth System Models (GSCE) (Shangguan *et al.*, 2014), according to the method of Torri, *et al.* (1997):

$$K = 0.0293 * (0.65 - Dg + 0.24 * Dg^2) * e^{\{-0.0021*\frac{OM}{f_{clay}} - 0.00037*\left(\frac{OM}{f_{clay}}\right)^2 - 4.02*f_{clay} + 1.72*f_{clay}^2\}} \quad (2)$$

where Dg is defined as:

$$Dg = -3.5 * f_{sand} - 2 * f_{silt} - 0.5 * f_{clay} \quad (3)$$

where fsand, fsilt and fclay are the fractions of respectively sand (particle size of 0.05-2mm), silt (particle size of 0.002-0.05 mm) and clay (particle size of 0.00005-0.002 mm). OM is the percent organic matter. Volcanic soils are defined as Andosols according to the FAO 90 in the Harmonized World Soil Database (HWSD), and are given a K factor value of 0.08. To account for the effect of stoniness on soil erosion we reduced the total erosion by 30% for areas with a gravel percentage larger or equal to 30% for nonagricultural land (Cerdan et al., 2010). For agricultural and grassland areas we reduced soil erosion by 80% in areas where the gravel percentage exceeded 12% (Doetterl et al., 2012).

The S factor of the adjusted RUSLE model is computed by the continuous function of Nearing (1997):

$$S = 1.5 + \frac{17}{1+e^{(2.3-6.1*\sin\theta)}} \quad (4)$$

where θ is the percent slope that is derived from a 1 km digital elevation model (DEM) and scaled to a resolution of 150m according to the fractal method presented by Naipal *et al.* (2015).

S2 Differences between the constrained and unconstrained PFT maps

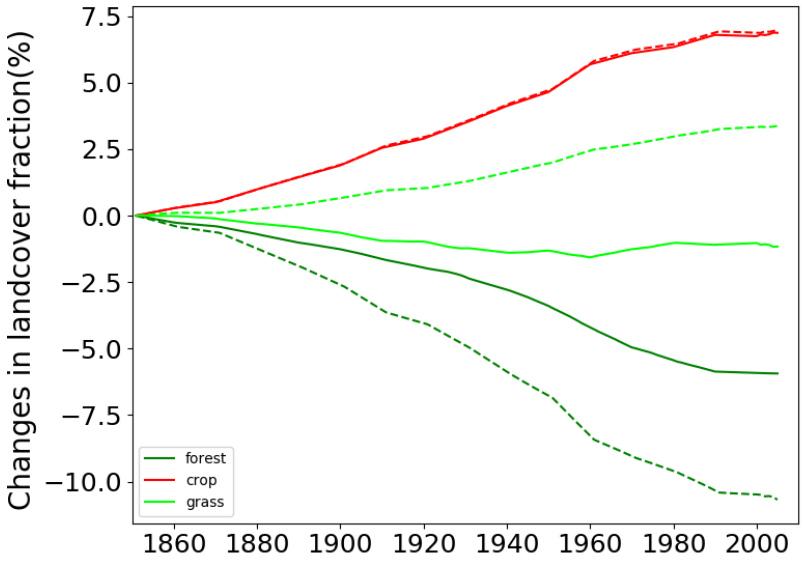

Figure S2: Changes (%) in forest (green), grass (light-green) and crop (red) fractions over the period 1850-2005 with respect to the year 1850AD. The dashed lines represent data from the unconstrained PFT map, while the straight lines represent data from the PFT map from Peng et al. (2017).

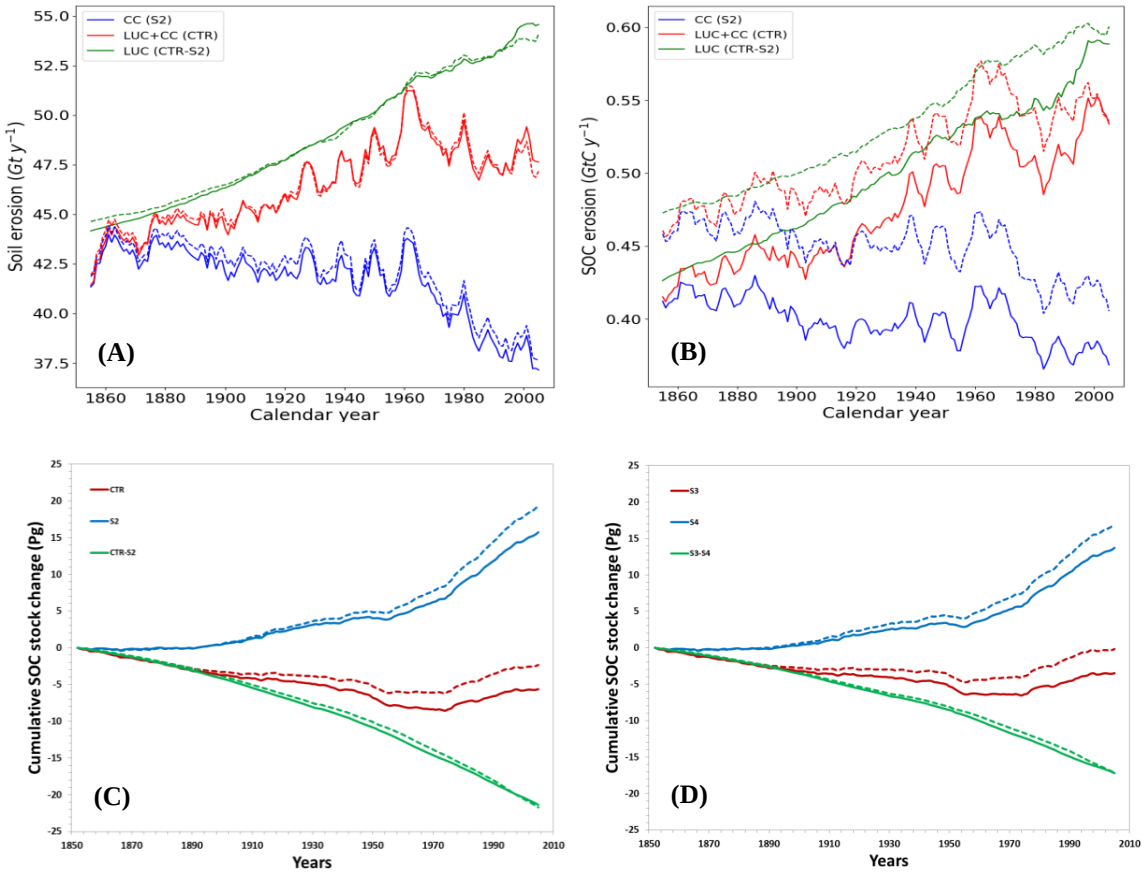

Figure S3: Differences in (A) soil and (B) SOC erosion rates and (C and D) cumulative SOC stock changes between the PFT map that is constrained by forest area data (straight lines) and the PFT map that is not constrained by forest area data (dashed lines).

65

S3 Variability in NPP, biomass and litter

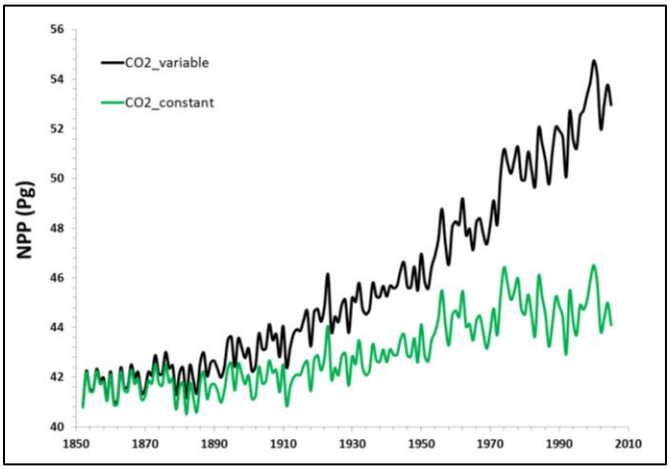

Figure S4: Global total NPP over the historical period from the "CO2_constant" simulation (green) and the "CO2_variable" simulations (black) using the full ORCHIDEE model

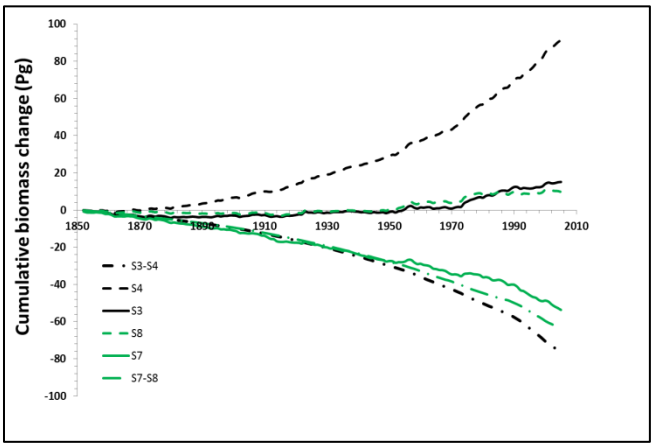

70

Figure S5: Cumulative historical changes in biomass from simulations with the emulator using variable atmospheric CO_2 (S3, S4, S3-S4), and using constant atmospheric CO_2 (S7, S8, S7-S8)

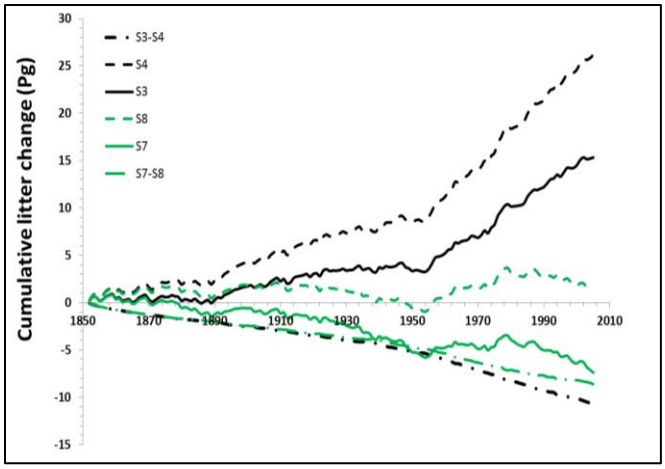

Figure S6: Cumulative historical changes in litter from simulations with the emulator using variable atmospheric CO_2 (S3, S4, S3-S4), and using constant atmospheric CO_2 (S7, S8, S7-S8)

S4 Comparison of SOC stocks of GSDE and the emulator

Figure S1 shows that our emulator, and the used version of the ORCHIDEE model in general, underestimates SOC stocks globally, except for the high-latitudes.

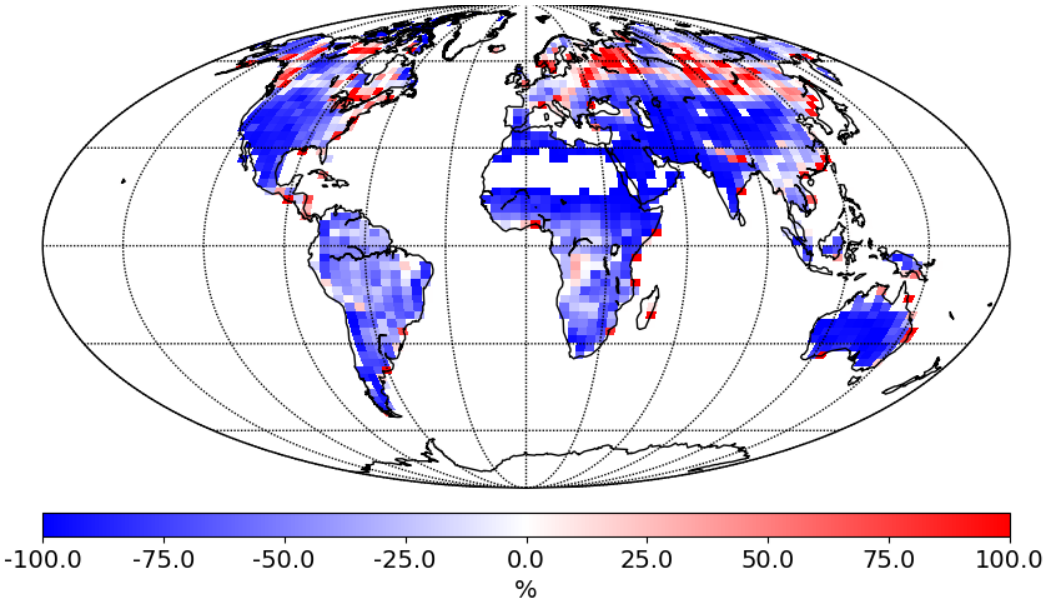

Figure S7: Difference between SOC stocks of the emulator (simulation S1) and the SOC stocks of GSDE as a percentage of the SOC stocks of GSDE till 2m depth. Red colors show larger SOC stocks by the emulator, while blue colors indicate smaller SOC stocks by the emulator compared to GSDE.

PFT number	PFT description	Area-weighted mean re
0	Bare soil	2.5
1	Tropical broad-leaved evergreen	0.72
2	tropical broad-leaved raingreen	1.33
3	temperate needleleaf evergreen	1.29
4	temperate broad-leaved evergreen	1.25
5	Temperate broad-leaved summergreen	1.09
6	boreal needleleaf evergreen	1.33
7	boreal broad-leaved summergreen	1.13
8	boreal needleleaf summergreen	0.93
9	C3 grass	2.03
10	C4 grass	2.3
11	C3 agriculture	0.73
12	C4 agriculture	0.78

Table S2: Global area-weighted average '*re*' values per PFT after calibrating the vertical discretization scheme of the emulator to have similar SOC stocks between the original ORCHIDEE model and the emulator without soil erosion and LUC.

PFT	r
Bare	5
Grass	4
Crop	4
Forest	1 or 0.8

Table S3: values of the r parameter (root profile ORCHIDEE)

References

Cerdan, O., Govers, G., Le Bissonnais, Y., Van Oost, K., Poesen, J., Saby, N., Gobin, a., Vacca, a., Quinton, J., Auerswald, K., Klik, a., Kwaad, F. J. P. M., Raclot, D., Ionita, I., Rejman, J., Rousseva, S., Muxart, T., Roxo, M. J. and Dostal, T.: Rates and spatial variations of soil erosion in Europe: A study based on erosion plot data, Geomorphology, 122(1–2), 167–177, doi:10.1016/j.geomorph.2010.06.011, 2010.

Doetterl, S., Van Oost, K. and Six, J.: Towards constraining the magnitude of global agricultural sediment and soil organic carbon fluxes, Earth Surf. Process. Landforms, 37(6), 642–655, doi:10.1002/esp.3198, 2012.

Frieler, K., Betts, R., Burke, E., Ciais, P., Denvil, S., Ebi, K., Eddy, T., Emanuel, K., Elliott, J., Galbraith, E., Simon, N., Halladay, K., Hattermann, F., Hickler, T., Hinkel, J., Mengel, M., Mouratiadou, I., Schmied, H. M., Vautard, R., Vliet, M. Van, Warszawski, L. and Zhao, F.: Assessing the impacts of 1 . 5 ° C global warming – simulation protocol of the Inter-Sectoral Impact Model Intercomparison Project (ISIMIP2b), Geosci. Model Dev. Discuss., (October), 1–59, doi:10.5194/gmd-2016-229, 2016.

Naipal, V., Reick, C., Van Oost, K., Hoffmann, T. and Pongratz, J.: Modeling long-term, large-scale sediment storage using a simple sediment budget approach, Earth Surf. Dyn., 4(2), doi:10.5194/esurf-4-407-2016, 2016.

Nearing, M. a.: A SINGLE, CONTINUES FUNCTION FOR SLOPE STEEPNESS INFLUENCE ON SOIL LOSS, Soil Sci. Soc. Am. J., 61(3), 1997.

Panagos, P., Borrelli, P., Meusburger, K., Alewell, C., Lugato, E. and Montanarella, L.: Estimating the soil erosion cover-management factor at the European scale, Land use policy, 48, 38–50, doi:10.1016/j.landusepol.2015.05.021, 2015.

Panagos, P., Borrelli, P., Meusburger, K., Yu, B., Klik, A., Lim, K. J., Yang, J. E., Ni, J., Miao, C., Chattopadhyay, N., Sadeghi, S. H., Hazbavi, Z., Zabihi, M., Larionov, G. A., Krasnov, S. F., Gorobets, A. V., Levi, Y., Erpul, G., Birkel, C., Hoyos, N., Naipal, V., Oliveira, P. T. S., Bonilla, C. A., Meddi, M., Nel, W., Al Dashti, H., Boni, M., Diodato, N., Van Oost, K., Nearing, M. and Ballabio, C.: Global rainfall erosivity assessment based on high-temporal resolution rainfall records, Sci. Rep., 7(1), doi:10.1038/s41598-017-04282-8, 2017.

Shangguan H.W., Dai Y., Duan Q., Liu B., Y. H.: A global soil data set for earth systemmodeling Wei, J. Adv. Model. Earth Syst., 6, 249–263, doi:10.1002/2013MS000293.Received, 2014.

Torri D., Poesen J., B. L.: Predictability and uncertainty of the soil erodibility factor using a global dataset, CATENA, 31, 1–22, 1997.

Walter H., Wischmeier, D. D. S.: Predicting RAINFALL-EROSION LOSSES FROM CROPLAND EAST OF THE ROCKY MOUNTAINS. Guide for Selection of Practices for Soil and Water Conservation, edited by A. R. Service, Washington D.C., 1972.